Effects of hyperfine structure on coherent excitation

Bruce W. Shore and Michael A. Johnson

Lawrence Livermore National Laboratory, University of California 94550

We point out how the presence of hyperfine structure can improve the coherent excitation and ionization of $J \to J-1$ and $J \to J$ transitions. In the limit of Rabi frequency dominating hyperfine splitting one recovers previously noted rules.

When one deals with coherent excitation, as described by a Schrödinger equation,[1] one often encounters bottlenecks which are not present in incoherent excitation, as described by rate equations.[2] One example of a bottleneck occurs in the excitation of degenerate levels,[3] as occurs when levels have angular-momentum quantum numbers $J \to J' \to J'' \to \cdots$. It is not difficult to show[1] that, for integer J, the sequence $J \to J+1 \to J+2 \to \cdots$ allows all of the ground sublevels to be excited, (and subsequently ionized) whereas in the sequence $J \to J \to J \to \cdots$ one sublevel does not participate in excitation and in the sequence $J \to J-1 \to J-2 \to \cdots$ each step diminishes the number of excited sublevels by two. (These observations apply either to linear polarization or to a succession of circular polarizations of the same sense. For half-integer J and linear polarization the sequence $J \to J \to J \to \cdots$ allows complete excitation.) These observations have nothing to do with details of the excitation process, such as excitation pulse shapes or the time dependence of excitation probabilities. The rules follow immediately from consideration of the excitation linkage patterns, and are based upon elementary selection rules.

The presence of hyperfine structure alters these selection rules and can allow, in some instances, complete excitation and ionization of sublevels which, in the absence of hyperfine structure, would remain in the ground state. Once again one can determine the number of inaccessible sublevels by considering the relevant linkage diagrams, as shown in Fig. 1 and 2. Here we have sketched, on the top row, linkage diagrams in the absence of nuclear spin. The diagram shows each of the magnetic sublevels and their interconnection by dipole transitions for linear polarization ($\Delta M_J = 0$) and for circular polarization ($\Delta M_J = 1$). These connections we shall call "allowed" linkages (i.e., allowed by dipole selection rules between unperturbed basis states); all other linkages are "forbidden". When we allow nuclear spin I to be nonzero, but do not allow any hyperfine interaction, then M_J remains a good quantum number, but each

M_J sublevel now has $2I+1$ sub-sublevels, which one can label by quantum number M_I. These are unchanged in transitions of the atomic-dipole moment. The central row of Figs. 1 and 2 illustrate this situation. The hyperfine interaction mixes states of different M_J and M_I, but it does not affect the sum $M_F = M_J + M_I$. Thus we can readily sketch a linkage diagram for weak hyperfine interaction by assuming that each unperturbed transition to a given sublevel $M_I M_J$ is apportioned amongst other transitions to the same value of M_F. The lowest row of graphs in Figs. 1 and 2 show the resulting linkages. It is now a simple matter to count the number of lower level sublevels which
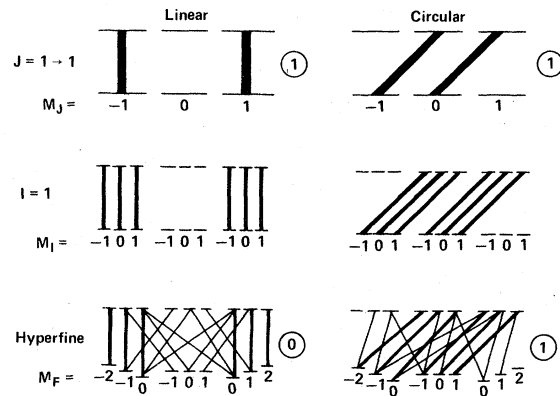

FIG. 1. Linkage pattern for $J = 1 \to 1$ transitions, showing dipole allowed connections between ground and excited sublevels. Left-hand patterns are for linearly polarized light ($\Delta M = 0$), right-hand patterns are for circularly polarized light ($\Delta M = 1$). Upper row shows cases without hyperfine structure ($I = 0$); sublevels are identified by M_J values. Middle row shows effect of nuclear orientation degeneracy with $I = 1$: each sublevel M_J now has $2I + 1 = 3$ sub-sublevels, identified by M_I. We here neglect hyperfine interaction, so sublevels are degenerate and atomic-dipole selection rule is $\Delta M_I = 0$. Bottom row shows effect of hyperfine interaction: energies are shifted and states are mixed. Strong lines show linkages allowed in the limit of zero hyperfine interaction; weak lines show linkages allowed by first-order perturbation theory.
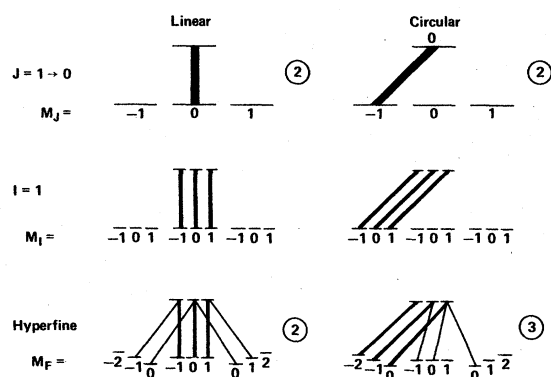
FIG. 2. As in Fig. 1 but for $J = 1 \rightarrow 0$ transition.

have no connection to excited sublevels; these numbers appear circled in Figs. 1 and 2. By inverting Fig. 2 we see that in transitions $J \rightarrow J + 1$ all lower sublevels ionize. Table I summarizes these results.

As one can see, the presence of hyperfine interaction can significantly diminish the fraction of inaccessible sublevels, e.g., from $2/(2J + 1)$ to $2/(2J + 1)(2I + 1)$ in the case of $J \rightarrow J - 1$ and linear polarization. However, although linkage diagrams allow one to determine the eventual fate of ionizable sublevels, they do not directly reveal the rate at which ionization occurs. To indicate the expected time dependence we have drawn the strongest transitions with heavy lines in Figs. 1 and 2. The light lines vanish in the limit of vanishing hyperfine interaction. Thus we expect, and quantitative analyses confirm, that as the hyperfine interaction diminishes one requires an increasingly long time to observe effects of the weak linkages. In the limit of vanishing hyperfine interaction one obtains the dynamics appropriate to a spinless nucleus.

The details of excitation and ionization dynamics depends upon the relative importance of the several interactions comprising the rotating wave approximation (RWA) Hamiltonian: the basic spinless free-atom Hamiltonian H^A (including ionization loss), the dipole-atom interaction H^D, and the nuclear hyperfine interaction H^N. When the effects

TABLE I. Number of unconnected lower-level sublevels.

	No hyperfine lin	cir	Hyperfine lin	cir
$J \rightarrow J - 1$	2	2	2	3
$J \rightarrow J$	1 $_{(0)}$[a]	1	0	1
$J \rightarrow J + 1$	0	0	0	0

[a] (0) for J = half odd integer.

of H^N are absent one deals with the Hamiltonian $H^O = H^A + H^D$ whose eigenstates are the dressed-atom states. Although H^D mixes states of different J and excitation, eigenvalues of H^O can be labeled with the M_J value appropriate to the lowest state of a linked sequence: Eigenvalues of H^O for the two-level sequences of Figs. 1 and 2 are $\pm (\hbar/2) \times \Omega(M_J)$, where $\Omega(M_J)$ is the Rabi frequency.

The presence of the hyperfine interaction H^N alters the dressed-atom states: The operator H^N mixes basis states of different M_J while preserving F and M_F as good quantum numbers ($\vec{F} = \vec{I} + \vec{J}$). When H^N is a small perturbation upon H^O it introduces a dependence upon M_J and M_I in the dressed-atom eigenvalues, having the form a $(M_I M_J) + b(M_I M_J)^2$. The perturbation is small if this hyperfine splitting is much smaller than the dressed-atom energy, i.e., smaller than the Rabi frequency. The mixing of states induced by H^N, as predicted by first-order perturbation theory, is proportional to a matrix element of H^N divided by the difference between two dressed-atom energies. Because the dependence of $\Omega(M_J)$ upon magnetic quantum number M_J (expressing relative orientation of dipole moment and laser electric field) occurs through a Clebsch-Gordan coefficient of order unity,[3] differences between various dressed state eigenvalues are roughly approximated by a root-mean-square (rms) Rabi frequency Ω^O. Thus the admixture of allowed linkage into an otherwise forbidden linkage grows roughly as the ratio of hyperfine splitting to Rabi frequency.

The effect of H^N upon the dynamics is as follows. For hyperfine splitting much less than the Rabi frequency, the atom behaves, over many Rabi cycles, as though it had zero nuclear spin. Only after a long time, i.e., many cycles, does the small admixture of states alter the dynamics by exciting and ionizing the forbidden linkages. Eventually, however, ionization will approach a completeness determined by the hyperfine connection diagrams of Figs. 1 and 2.

When the hyperfine splitting becomes comparable to the Rabi frequency (in some mean sense; there are $2F + 1$ hyperfine splittings and $2J + 1$ Rabi frequencies) the mixing of sublevels becomes sufficiently great that one cannot distinguish "allowed" from "forbidden" linkages, and the excitation and ionization of all connected hyperfine sublevels proceeds within a few Rabi cycles. When the hyperfine splitting greatly exceeds the Rabi frequency one deals with H^D as a perturbation upon $H^1 = H^A + H^N$. The hyperfine splitting here produces a detuning which impedes excitation. Here again many Rabi cycles must occur before the detuned transitions can produce appreciable ionization.

This reasoning shows that for given hyperfine

structure there is an optimum choice of excitation intensity: When the intensity is too weak the hyperfine detuning slows the excitation, whereas when the intensity is very strong the excitation of forbidden linkages requires many Rabi cycles.

We have described the interplay of H^A, H^D, and H^N in a basis characterized by quantum numbers M_J and M_I, as is appropriate to $H^O = H^A + H^D$ as the unperturbed Hamiltonian. One will, of course, obtain the same results in any other basis, e.g., a basis characterized by F and M_F appropriate to $H^1 = H^A + H^N$ as the unperturbed Hamiltonian. That is, the excitation probability from initial level n to level n' after time t is expressible as

$$p(n \to n' \,|\, t) = \frac{1}{\tilde{\omega}} \sum |\langle n' M'_J M'_I | \, U(t) \,| n M_J M_I \rangle|^2$$

$$(1a)$$

$$= \frac{1}{\tilde{\omega}} \sum |\langle n' F' M'_F | \, U(t) \,| n F M_F \rangle|^2,$$

$$(1b)$$

where $\tilde{\omega} = (2J + 1)(2I + 1)$ is the statistical weight of the initial level. Here $U(t)$ is the time-evolution operator and the sums go over $M_J M_I M'_J M'_I$ in the first instance and over $F M_F F' M'_F$ in the second instance.

Formula (1) tells us to carry out a succession of $\tilde{\omega}$ independent calculations, beginning in each case at time $t = 0$ in a different basis state. We then sum the squares of transition amplitudes to each possible final state. The equality of Eqs. (1a) and (1b) is a consequence of the existence of a unitary transformation between bases.

Although observable results do not depend upon our choice of basis states, the linkage patterns appear differently in the two coupling schemes. For example, Fig. 3 shows the linkages for the $J = 1 \to 1$ transitions, with $I = 1$, which appear in Fig. 2. Although it might appear that all of the sublevels would become excited, even in the absence of hyperfine splitting, such is not the case.
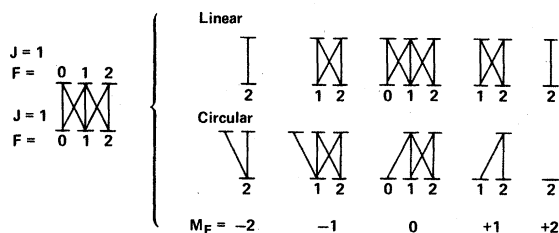

FIG. 3. Linkage patterns for $J = 1 \to 1$ transitions with $I = 1$ using $F M_F$ labels instead of $M_J M_I$ labels of Fig. 1. Each pattern at the right corresponds to a different M_F value; the pattern at the left shows linkages summed over M_F values. Labels 0, 1, and 2 on each pattern identify F values.

One must keep in mind the fact that coherent excitation preserves phase relationships. Thus one must associate a phase with each of the linkages of Figs. 1 – 3, thereby allowing destructive interference. In the absence of hyperfine splitting, the transitions of Fig. 3 can be transformed (via angular-momentum recoupling) into the transitions in the center of Fig. 2; destructive interference prevents complete ionization of all the linked sublevels of Fig. 3. Hyperfine splitting breaks the degeneracy of the sublevels and thereby overcomes the destructive interference. Mathematically speaking, some of the matrices of $H^O = H^A + H^D$ in the degenerate $F M_F$ scheme have null eigenvalues even when H^A includes loss; hence there are components which never ionize. The presence of H^N introduces finite loss rates on all eigenvalues.

ACKNOWLEDGMENTS

[1] B. W. Shore and M. A. Johnson, J. Chem. Phys. 68, 563 (1978).

[2] J. R. Ackerhalt and B. W. Shore, Phys. Rev. A 16, 277 (1977).

[3] B. W. Shore, Phys. Rev. A 17, 1739 (1978).